Induced velocity model in steep descent and vortex-ring state prediction

Jérémy JIMENEZ

André DESOPPER, Armin TAGHIZAD and Laurent BINET

Laboratoire ONERA-École de L'Air
Base Aérienne 701
13661 Salon Air - France

Steep aproaches will play an important role in the near future helicopter missions in particular for noise reduction, however, in steep descent the helicopter flight envelope is limited by the region knowned as *vortex-ring state*. Entering this area, while flying close to the ground, can be extremely dangerous. Indeed, the vortex-ring state was implicated in 32 helicopter accidents between 1982 and 1997 [1].
The objective of this work is to predict the vortex ring state limits and to model helicopter behaviour during steep approach.
Because of the importance of induced velocity in helicopter flight simulation code, an empirical Vim model is developed. First momentum theory is extented to all flight configurations. Then the computed Vim is adjusted to experimental data available, multiplying by a coefficient that takes into account different losses that occur in descent flight.
An analytical criterion predicting the vortex ring state limits is proposed. This criterion is founded on Wolkovitch theory [2] which is improved in order to take into account the wake skew angle. In addition, this criterion is applied using the developed Vim model instead of momentum theory.
Finally, the vortex ring state is modeled, breaking down into two aspects. In one hand, the flow fluctuations that occur in vortex ring state are modeled using the previous criterion to estimate their intensity. On the other hand, flight tests performed at CEV have exhibited particular Vz responses to collective inputs including power settling. Eurocopter flight mechanics code HOST improved with the proposed Vim model reproduced well these characteristic phenomena of the complex vortex ring state.

Notations

c mean chord of the rotor blade, m

DT0 collective pitch angle, deg

Fz rotor thrust, N

Nz normal load factor

Pn_o hover required power, kW

P_w required power, kW

R rotor radius, m

Vi_o hover induced velocity, $m.s^{-1}$

Vim mean induced velocity, $m.s^{-1}$

Vh horizontal velocity, $m.s^{-1}$

Vs slipstream velocity, $m.s^{-1}$

V_{tv} tip vortices velocity, $m.s^{-1}$

Vx inplane velocity component, $m.s^{-1}$

Vz normal velocity component, $m.s^{-1}$

$\bar{\eta}$ normalized axial flow

$\bar{\mu}$ normalized inplane flow

$\bar{\nu}$ normalized induced flow

χ wake skew angle, deg

ρ air density, $kg.m^{-3}$

ϕ roll attitude, deg

θ pitch attitude, deg

ψ azimuth, deg

$\beta 0$, $\beta 1c$, $\beta 1s$ rotor flapping angle, deg

Ω rotational velocity of the rotor, $rad.s^{-1}$

Introduction

Steep descent is an important flight phase as well for civil helicopters for which new steep approach procedures will be used notably for noise reduction as for military ones requiring the capability of approaching and landing short or enrering a confined area for any rescue operation. However, in steep descent the flight envelope is limited by the region of *vortex ring state*. The turbulent circulating air existing in this particular state can cause serious handling difficulties that frequently leads to temporary loss of helicopter control. Entering this area, while flying close to the ground, can be extremely dangerous. Indeed, the vortex-ring state was implicated in 32 helicopter accidents between 1982 and 1997 [1].

One challenge, in the near future, would be the improvement of rotorcrafts handling qualities at high glide slope approaches, via appropriates control laws associated to carefree handling means (active side-sticks, HUD). The design and the development of this kind of systems require a good knowledge of helicopter flights mechanics in this specific flight configuration.

Because of the importance of induced velocity in helicopter flight simulation, first an empirical Vim model is developed. Then a criterion predicting the vortex ring state limits is proposed. An induced velocity fluctuations model has also been developed. Finally, the mean features of the vortex state (parameters fluctuations and particular Vz responses) are reproduced with Eurocopter flight mecanics code HOST (Helicopter Overall Simulation Tool). This results are compared with flight test data performed with the instrumented DAUPHIN 6075 in service in the French Flight Test Centre (CEV).

1 Induced velocity model

All existing induced velocity models used in flight mechanics codes are founded on a mean component, generally computed by simple momentum or vortex theory. Because these theories are not valid in descent flight, many models were elaborated for such conditions. Most of them only holds in vertical descent, as a result of the axis-symmetrical flow that simplifies the problem in that case. The differences between the methods used show that the problem remains still misunderstood. Despite many models are available in vertical descent, until now, no physical model exists in the general case of descent with forward flight. An empirical approach is elaborated in order to compute Vim in all flight conditions, including descent in forward flight.

1.1 Momentum equation

Both momentum and simple vortex theory provide the following equation:

$$F_z = 2.\rho.\pi.R^2.V_t.V_i \qquad (1)$$

with $V_t = \sqrt{{V_x}^2 + (V_i + V_z)^2}$, the wake transport velocity.

Equation (1) may be nondimensionalized by dividing both sides by the hover induced velocity Vi_o, to yield:

$$1 = \bar{\nu}^2[\bar{\mu}^2 + (\bar{\nu} + \bar{\eta})^2] \qquad (2)$$

1.2 Momentum improvement in vertical descent

Figure 1 shows the solution of equation 2 in vertical descent ($\bar{\mu} = 0$) and compares them with experimental data from [3]. The momentum induced velocity follows and minimizes the experimental data for -1.5<$\bar{\eta}$ < 0 and for $\bar{\eta} < -2$. Between $\bar{\eta} = -1.5$ and $\bar{\eta} = -2$ the experimental values link the upper and lower branches of momentum theory.

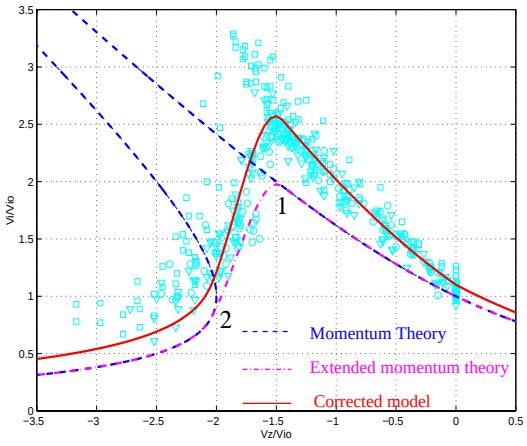

Figure 1: Normalized induced velocity in vertical descent

This region where solutions of (2) are erroneous corresponds to a surrounding area of the ideal autorotation for which $\bar{\eta} = -\bar{\nu}$. In this situation, the normalized induced velocity tends towards infinity in order that the right side of equation (2) keep a constant value. The finite experimental values of $\bar{\eta}$ means that a term is deficient in equation (2). Physically, this term could represent the drag of the rotor in autorotation as mentioned by

Drees [4]. Here, the induced velocity was calculated using an interpolating method inspired by the works of Baskin and al [5].

Let $\bar{\eta}_1$ and $\bar{\eta}_2$ be the critical normalized rates of descent surrounding the ideal autorotation and $\bar{\nu}_1$ and $\bar{\nu}_2$ be the corresponding normalized induced velocities computed by equation (2). The expression of the derivative is not easy to be obtained because $\bar{\nu}$ is computed numerically by solving equation (2) but no expression giving $\bar{\nu}$ as a function of $\bar{\eta}$ et $\bar{\mu}$ is available. Nevertheless, Peters and Chen [6] have shown that:

$$\frac{\partial \bar{\nu}}{\partial \bar{\eta}} = -1 \pm \frac{1}{\bar{\nu}^3} \frac{1}{\sqrt{\frac{1}{\bar{\nu}^2} + \mu^2}}$$

giving respective values of $(\frac{\partial \bar{\nu}}{\partial \bar{\eta}})_1$ and $(\frac{\partial \bar{\nu}}{\partial \bar{\eta}})_2$ in $\bar{\eta}_1$ and $\bar{\eta}_2$. So, four conditions allow to interpolate the normalized induced velocity between point 1 and 2 (figure 1) with a 3^{rd} order polynomial function. For $\bar{\eta} < -\bar{\eta}_2$, only the lower solution of equation (2) is considered.

Normalized induced velocity calculated in that way in vertical descent is represented in figure 1. The calculated values follow and minimize the experimental ones over the all range of descent.

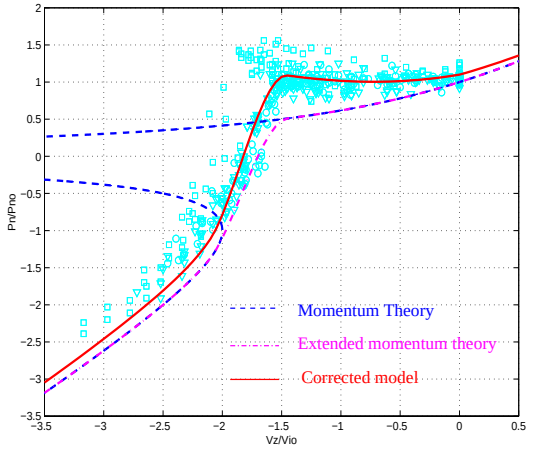

Figure 2: Normalized required power in vertical descent

The extended momentum theory provides a lower bound for the induced velocity. The results obtained with this method in term of required power (figure 2) shows that the extended momentum theory represent the optimum performance of the rotor because the calculated required power minimized the experimental one (2). Heyson [7] and Drees [4] assumes that this idealized picture of rotor performance comes from the omission of viscous losses and all losses caused by nonuniformity of momentum transfert. Figures 1 and 2 show also the results obtained by the previous model with a multiplicative coefficient k_{Vi} which takes these different losses into account.

1.2.1 Descent in forward flight

The same method is applied to the descent in forward flight with interpolation limits $\bar{\eta}_1$ and $\bar{\eta}_2$ and a coefficient k_{Vi} adjusted to the normalized forward speed $\bar{\mu}$. Beyond a critical value $\bar{\mu}_{crit}$ the normalized induced velocity is computed by equation 2 again for any value of $\bar{\eta}$ (figure 3). As the model is extrapolated when $\bar{\mu} \neq 0$, more experimental data are needed to update vertical measurements and to extend them to forward descent.

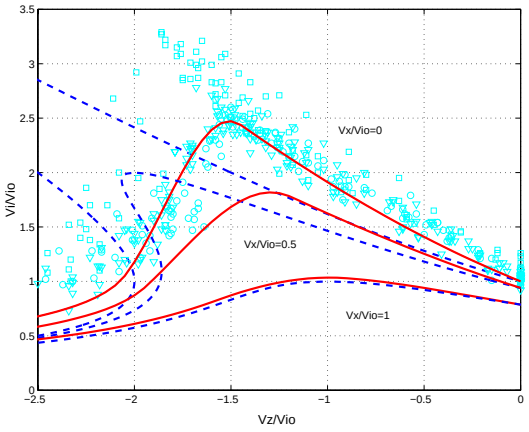

Figure 3: Normalized induced velocity in forward flight

The model has been implemented in the Eurocopter flight mecanics code HOST. The last chapter will show that the corrected model improved greatly the code, reproducing the mean features of vortex ring state.

2 Vortex ring state prediction

Even if all helicopter world actors know the vortex-ring state, the phenomenon remains still misunderstood and the helicopter flight envelope in descent remains not correctly estimated. Previous experimental studies of the vortex ring state present different aspects of the phenomenon:

- Circulatory flow shown by visualisation, both in wind tunnel [8] and flight test [9],
- Unsteady flow exhibited by wind tunnel measurements [10] involving flight instabilities,
- Ct reduction at constant collective pitch shown in wind tunnel [10].

All these different aspects are connected. Indeed, the circulatory flow provides an induced velocity augmentation and flow fluctuations. Moreover, the Ct reduction is due to Vi increase that decreases local angles of attack.

From the pilot point of view, that can be characterized by turbulence and sudden increase of the rate of descent.

It is proposed, first to determine the limits of the region of roughness, then to generate flow fluctuations and finally to analyze phenomena implying the specific Vz evolution in descent flight.

2.1 Wolkovitch criterion [2]

The flow model considered by Wolkovitch consists of a slipstream with uniform flow at any section, surrounded by a protective tube of vorticity which separate the slipstream from the relative wind. This tube is made up by the tip vortices leaving the rotor and it is postulated that the unsteady vortex ring flow is associated with a breakdown in this protective sheath of vorticity. Wolkovitch assumes that the velocity of the vortex cores is the mean between velocities inside and outside the tube (figure 4). Moreover, the vortex ring state is supposed to occur when the relative velocity of the tip vortices falls to zero. This leads to the criterion for the upper limit:

$$\bar{\eta} = -\frac{\bar{\nu}}{2}$$

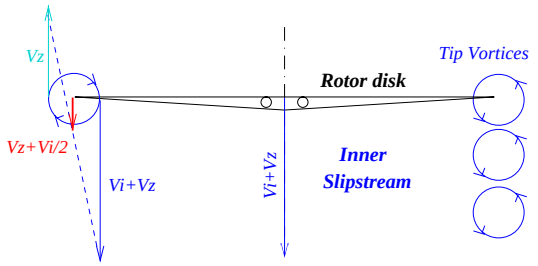

Figure 4: Wolkovitch flow model

For the lower limit, Wolkovitch used a coefficient k_W that take into account the distance above the rotor where the "pile-up" of vorticity occurs. The lower limit is then defined by:

$$\bar{\eta} = -\frac{k_W.\bar{\nu}}{2}, \quad 1 \leq k_W \leq 2$$

The recommended value of k_W is 1.4.

Figure 5 represents the limit obtained with this criterion ($k_W = 1.4$) where the induced velocity is computed by momentum theory.

The limits obtained are close to the experimental ones at low advance ratio. Nevertheless, the

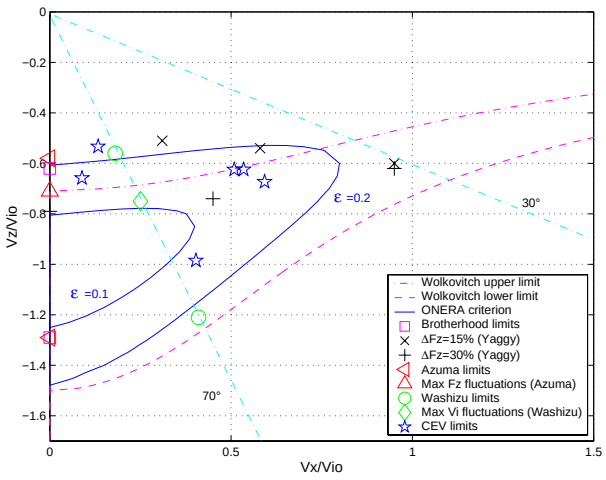

Figure 5: Vortex ring state limits

criterion predicts vortex ring state even for high advance ratios. This is consistent with neither experience nor the physical mechanisms that causes the vortex ring state.

2.2 Improved Wolkovitch model

As was mentioned by Peters and Chen [6], the deficiency of the previous theory comes from the fact that the wake skew angle is not considered in the wake geometry. In order to take into account the skew angle χ the flow model shown in figure 6 is used.

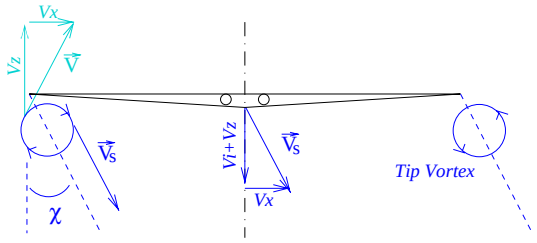

Figure 6: Flow model in forward descent

The tip vortices velocities $\overrightarrow{V}_{tv}$ is supposed to be again the mean between the velocities outside and inside the slipstream but owing to the wake skew angle χ:

$$\overrightarrow{V}_{tv} = \frac{1}{2}.(\overrightarrow{V} + \overrightarrow{V}_s) = \begin{pmatrix} V_{tv_x} \\ V_{tv_z} \end{pmatrix} = \begin{pmatrix} Vx \\ \frac{Vi}{2} + Vz \end{pmatrix}$$

Normalizing by the hover induced velocity:

$$\overrightarrow{\bar{V}}_{tv} = \begin{pmatrix} \bar{\mu} \\ \frac{\bar{\nu}}{2} + \bar{\eta} \end{pmatrix}$$

Unlike Wolkovitch, a single condition is used to predict vortex ring state limit that supposes the

unsteady flow associated with vortex ring state occurs when the tip vortices stand in the vicinity of the rotor. In other words, the rotor is in vortex ring state when the initial velocity of tip vortices is not large enough to carry them far from the rotor disk. This would lead to the following criterion:

$$|\vec{V}_{tv}| = \sqrt{V_{tv_x}^2 + V_{tv_z}^2} < \varepsilon$$

This criterion gives good results near vertical descent but doesn't match very well with experimental data from [8] and [11] when $\bar{\mu} \neq 0$. That is due to the fact that the normalized axial and inplane flows don't play a symetric role as figure 7 shows.

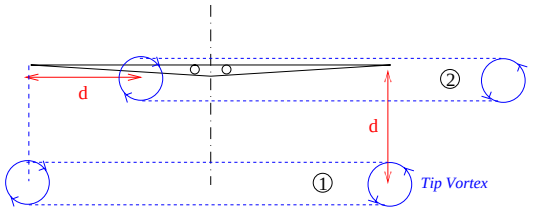

Figure 7: Physical difference between axial and inplane flow

Let's consider ① and ② as two vortex rings leaving the rotor at the same velocity, moving respectively in the axial and inplane direction. After a time t, the vortices have both covered the distance d but figure 7 shows that tip vortex ② is still in contact with rotor while vortex ① no longer interact with the rotor disk. As a result, the rotor is supposed to be in vortex ring state when:

$$\begin{cases} V_{tv_x} \leq \varepsilon_x \\ V_{tv_z} \leq \varepsilon_z \end{cases} \qquad (\varepsilon_z < \varepsilon_x)$$

Putting $\varepsilon_x = k.\varepsilon_z = k.\varepsilon$ with $k > 1$, the criterion become[1]:

$$\sqrt{(\frac{\bar{\mu}}{k})^2 + (\frac{\bar{\nu}}{2} + \bar{\eta})^2} \leq \varepsilon \qquad (3)$$

In the previous criteria ([2] and [6]), induced velocity was calculated with momentum theory which is not valid in descent. Here $\bar{\nu}$ is computed with the induced velocity model described above which is adapted to descent flight.

Value of coefficient $k = 4$ is chosen to match with experimental domains from [8] and [11]. The value of ε traduces the intensity of the vortex ring state fluctuations. Figure 5 represents the limits obtained with $\varepsilon = 0.2$ and $\varepsilon = 0.1$, that corresponds respectively to light and severe fluctuations levels. Flight test have been performed with the instrumented DAUPHIN 6075 in service in the French Flight Test Centre (CEV) to get the vortex ring state limits in flight. First data obtained are represented on figure 5 also with experimental data reported by [12].

[1] Newman et al [12] have also considered such coefficient

Dimensional limits: The physical limit is obtained by multiplying the normalized domain by $Vi_o = \sqrt{\frac{F_z}{2.\rho.\pi.R^2}}$. Consequently, the vortex ring state dimensional domain depends on:

- F_z approximately equivalent to the helicopter mass,
- R expressing the rotor dimensions,
- ρ expressing flight conditions.

Figure 8 compares the limits obtained for the DAUPHIN at two different masses.

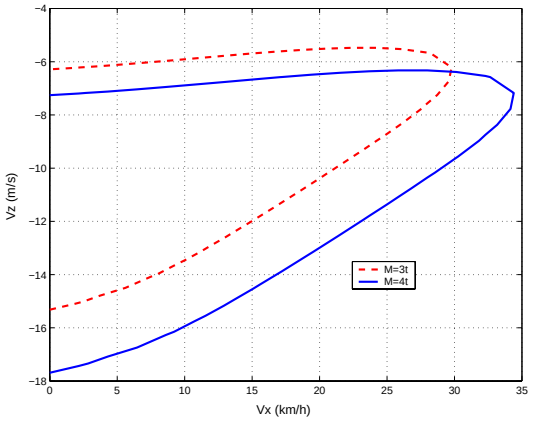

Figure 8: Helicopter mass influence on the vortex ring state domain

Axis influence: Rigorously criterion (3) must be applied in rotor axis. Trim calculations realized with Dauphin 365N at $z = 0m$, using HOST code, give the limit represented on figure 9. Simple multiplication of criterion (3) by Vi_o applied directly in helicopter axis is also represented. Because of small values of the helicopter pitch angles in these flight conditions, figure 9 shows little differences beetween the two limits. As a result, the simple criterion (3) can be used in helicopter axis multiplying by the hover induced velocity.

2.3 Application of the criterion to D6075 vortex-ring state flight

During engine failure flight tests, DAUPHIN 6075 encountered accidentally the vortex-ring state.

Figure 10 shows that the helicopter enters the vortex-ring state when its forward speed (UAa)

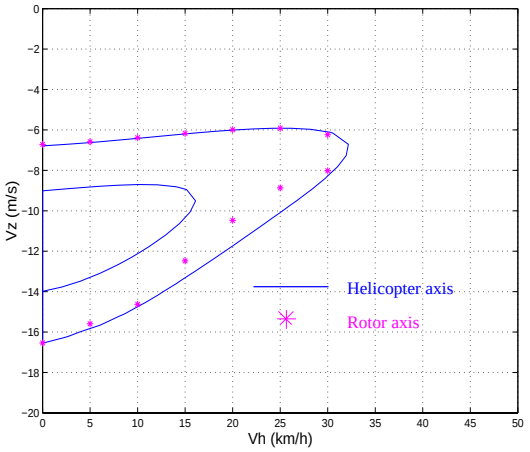

Figure 9: Comparison of vortex domains expressed in rotor and helicopter axis (m=3500kg, z=0m)

dropped while the pilot tries to reduce the descent rate (WAa) (between points 1 and 2). This maneuver implies a decrease of the criterion value that reaches 0.2 at point 2 and 0.1 at point 3, signifying an augmentation of vortex ring state intensity, that leads in a sharply Vz decrease. Next the helicopter leaves vortex ring state area by increasing its forward speed that augments the criterion value (0.2 at point 4). In this way, the pilot manages to stabilize and next to increase Vz. The bottom diagram shows a good correlation between the flight test beginning of Vz decrease and proposed limit.

3 Helicopter behaviour prediction in vortex ring state

3.1 Flow fluctuations

Method: As wind tunnel test exhibited a high level of flow fluctuations during the vortex ring state, it has been decided to introduce Vi fluctuations in HOST code. Moreover, measurements of Fz spectrum is available in literature [13]. This experimental spectrum obtained from a model rotor is first sampled and then is adapted to the Dauphin rotor with the help of the normalized frequency: $\omega_0 = \frac{\Omega.R}{c}$. However, this spectrum corresponds to a single flight condition ($\bar{\mu} = 0$, $\bar{\eta} = 0.75$) near maximum fluctuations level.

Yet, criterion (3) gives not only the limit of vortex ring but permits above all to estimate the intensity of fluctuations. Indeed, the value of the left side of equation (3) gives the intensity of fluctuations. More low is the value of criterion more important the fluctuations will. Accordingly, the spectrum is interpolated over vortex domain with

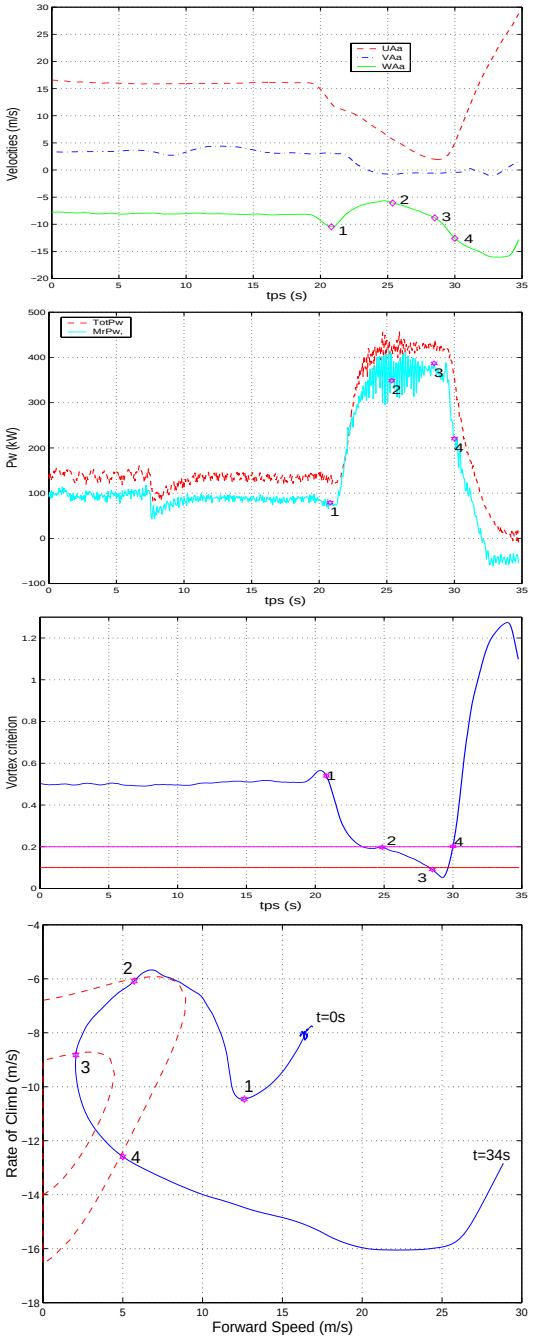

Figure 10: Main flight parameters and vortex ring state criterion during D6075 vortex-ring state flight

criterion (3) supposing that excited frequencies are the same on the whole domain.

As Fz fluctuations is a consequence of Vi fluctuations, a fluctuating term $\tilde{Vi}$ is added to the induced velocity. In view of the experimental Fz spectrum form, $\tilde{Vi}$ is chosen to be pseudo-harmonic:

$$\tilde{Vi} = \sum_{i=1}^{n} Ai. \cos\left(\omega_i.t + \phi_i\right)$$

The Fz spectrum obtained by simulation is then analyzed and compared with experimental one. Next, $\tilde{Vi}$ must be adjusted, through Ai and ω_i in order that computed spectrum matches with experimental one. The phase ϕ_i is a random number taken between 0 and $2.\pi$.

Figure 11 represents comparison between thrust fluctuations intensity computed with the model, some experimental data [10] and Euler numerical simulation [14]. In all the cases, a maximum of fluctuation of 12-14% of the mean thrust $\bar{F}z$ appears near $\bar{\eta} = -1$.

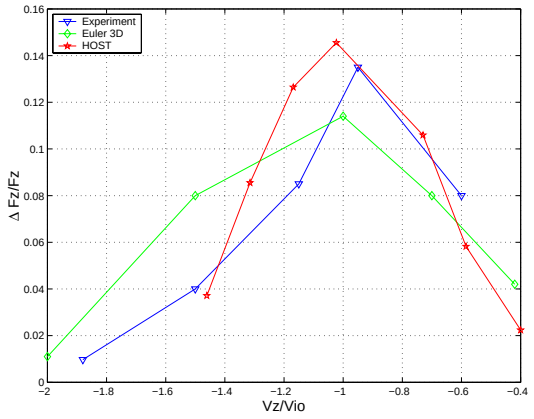

Figure 11: Comparison between thrust variation computed, experimental data and Euler numerical simulation in vertical descent

Figure 12 validates the model in term of frequencies, showing in one hand the experimental spectrum deducted from [13] and on the other hand the spectrum computed by HOST simulation.

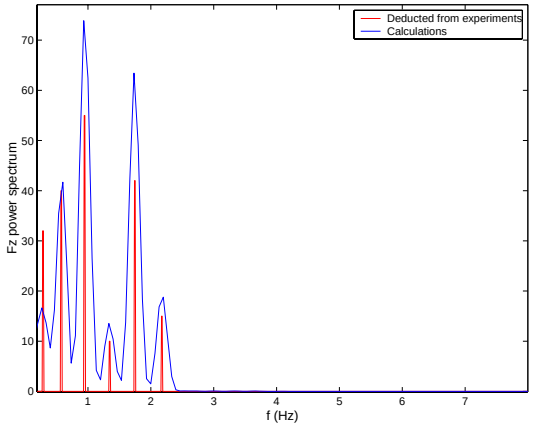

Figure 12: Comparison between experimental and calculated spectrum

Consequences: Figure 13 represents a simulation realized at Vh=10km/h, Vz=-10m/s and controls fixed. It is to note that the Vi fluctuations directly act on Fz and on the blade flapping angles. Whereas the fuselage attitude angles (ϕ, θ) present lower frequencies due to damping that acted between the rotor and the fuselage. The vertical speed Vz and the normal load factor Nz are also modified by Vi fluctuations.

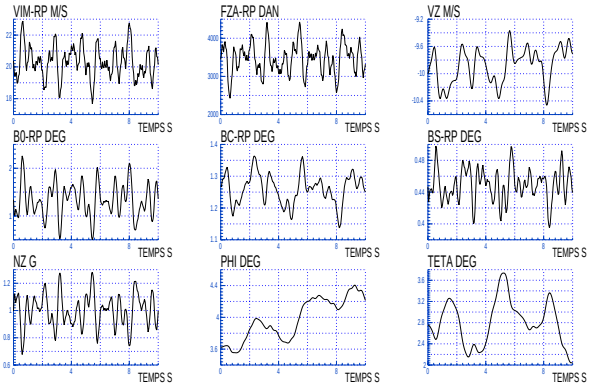

Figure 13: HOST simulation for Dauphin 365N (Vh=10km/,Vz=-10m/s), controls fixed with Vi fluctuations

Conclusion: Flow fluctuations has been modeled in the code HOST with an experimental spectrum [13] measured on a single point and interpolated over the whole vortex ring state domain with criterion (3). The excited frequencies are supposed to be constant on the whole vortex domain. More experimental data are needed to validate this hypothesis and to corroborate the spectrum form.

3.2 Vz response to collective pitch in descending flight

Vortex ring state can be quite dangerous because of the amazing Vz responses to DT0 implying sudden Vz fall. Flight tests, performed at the french flight test centre (CEV), exhibit such characteristic phenomena. The simple Vim model described above permits to reproduces qualitatively this Vz responses.

3.2.1 Vz response to DT0 reduction

Such an example is shown on figure 14. The pilot decreases progressively the collective pitch. First, Vz responses "normally" to DTO inputs: the two first DTO reductions of about $-0.2°$ produce a Vz decrease of about 2.5m/s. The third DTO reduction rather smaller than the previous ones leads to a descent rate higher than 15m/s.

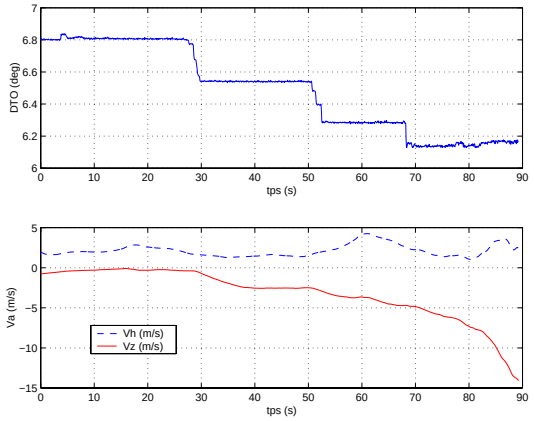

Figure 14: Flight test example of Vz response to collective pitch reductions

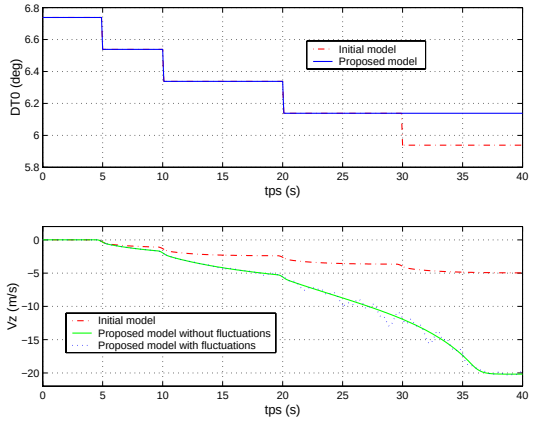

Figure 15: HOST calculations of Vz response to collective pitch reductions

The explanation of this phenomenon comes from the evolution of DT0 as function of Vz (figure 16). This curve presents a local minimum near Vz=- 6.5 m/s (point A). Between hover contition and this local minimum, Vz response is approximately a linear function of DTO inputs. Close to point A (on the hover side), any light DT0 reduction will imply new trim condition corresponding to Vz greater than those of point B. It is to note that segment [AC] represents an instable region.

A HOST simulation reproducing this phenomenon is shown on figure 15 with and without induced velocity fluctuations. Simulation with the initial Vim model is also indicated. With the initial model, no sudden Vz fall is visible, because of the uniform decrease of DTO with descent rate increase. With the proposed model a large increase of the descent rate is obtained as in the flight tests.

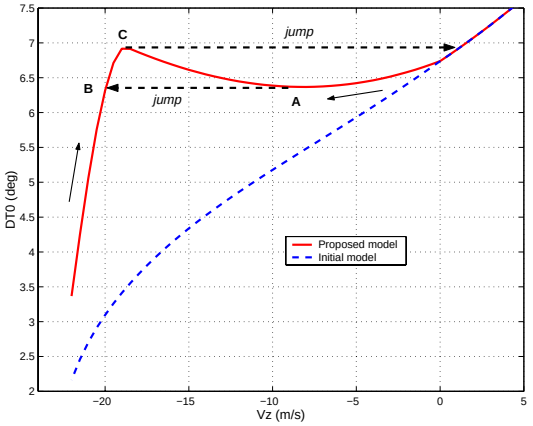

Figure 16: DT0 versus Vz in vertical flight (HOST trim calculations)

3.2.2 Vz response to DT0 increase: Power-settling

Power-settling is another important phenomenon occurring during descent flights. This phenomenon still misunderstood could be defined as an insensitivity of Vz to collective pitch increase.

DT0 increase within vortex ring state: Figure 17 exhibits a flight test illustrating this phenomenon. The Helicopter enters the vortex ring state by a deceleration, implying an augmentation of the rate of descent. At $t \approx 14.5s$ the pilot increases DT0 in order to stabilize Vz. Despite this DT0 increase ($+1^0$), Vz continue to fall during 5s stabilizing at $Vz \approx -12m/s$.

This phenomenon could be explained with the help of figure 16. Supposing that the helicopter is in a flight condition somewhere between points A and B. If the collective pitch is increased at a value smaller than those at point C, the helicopter will go to a trim condition situated on the stable part of the curve, between points B and C.

Such phenomenon is reproduced qualitatively with HOST simulation using the proposed Vim model as shown on figure 18. Beginning at Vz=-6m/s, the rate of descent increases in response to the DT0 decrease, tempting to reach the new trim position (beyond point C on figure 16). At t=8s, DT0 is increased to its initial value. Instead of going back to its first value (Vz=-6m/s), the rate of descent goes to the second trim position, situated between B and C on figure 16. With the initial model, the helicopter comes back to Vz=-6m/s.

DT0 increase beyond vortex ring state: The "jump" phenomenon also exists when the helicopter crosses the vortex ring state starting from

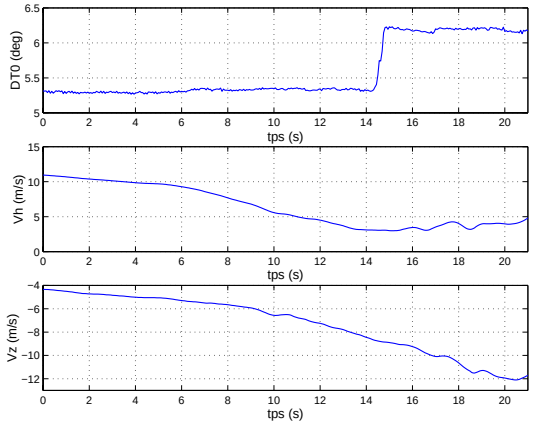

Figure 17: Flight test example of power settling

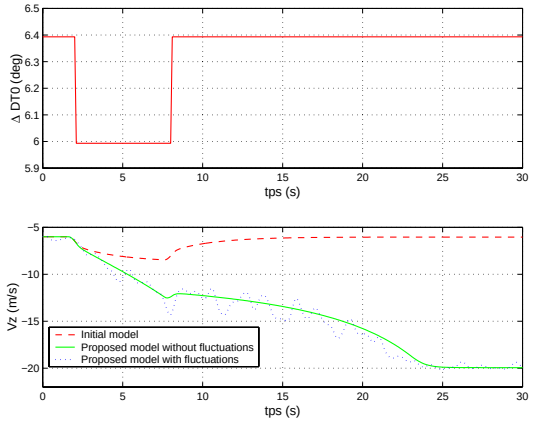

Figure 18: HOST simulation of power settling in vertical descent

a high rate of descent. However, this is more difficult to exhibit in flight. Because of the large Vz, the pilot has to increase DT0 rather quickly and it is difficult to realize step inputs. Figure 19 shows a flight test starting at $Vz \approx -20m/s$ and $Vh \approx 8m/s$. The pilot augments DT0 in order to decrease the rate of descent. At t=50s, Vz only reaches $\approx -15m/s$ despite a collective increase of about $+4°$. Beyond t=50s collective pitch is still slightly increases ($\simeq 0.2°$) and Vz increases sharply (about 10m/s in 10s).

Supposing a trim position at a rate of descent greater than the one at point B on the DT0 curve of figure 16 (between autorotation and point B). If DT0 is increased at value smaller than those at point C, the trim position moves upward. Taking into account the slope of the curve between autorotation and point C, the difference of Vz between the two trim positions will be small. When DT0 is increased at a value greater than those at point C, the Vz will increase, going to positive value.

Such phenomenon is reproduced with HOST calculations on figure 20.

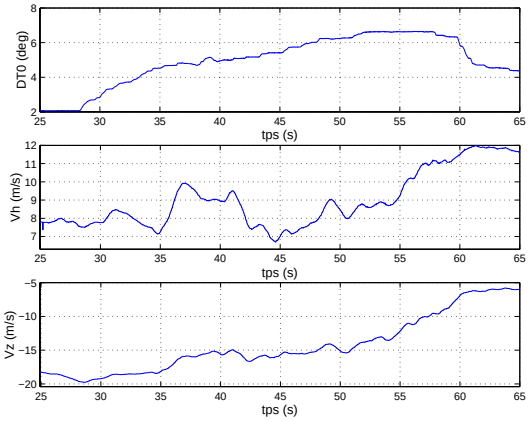

Figure 19: DT0 increase flight test

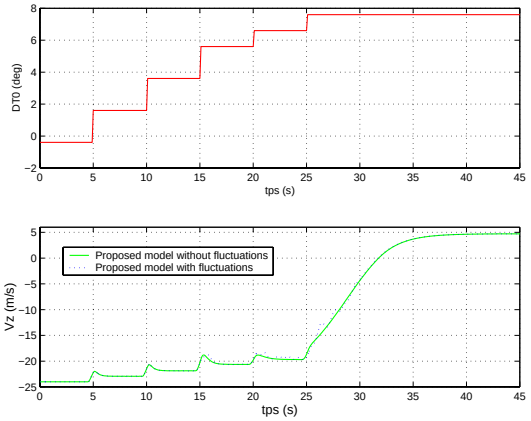

Figure 20: HOST simulation of DT0 increase beyond vortex ring state in vertical descent

Conclusion: Mean features of the complex vortex ring state including collective pitch insensibility (power settling) can be reproduced with a simple Vim model. Theoretical study as well as flight tests show that segment [AC] represents an instable region.

Conclusion

The induced velocity model elaborated improves greatly HOST code predictions. The mean characteristics of the vortex ring state observed during experimental studies are well reproduced. Both D6075 flight test and HOST calculations have demonstrated that vortex ring state can be considered as an instable region. The Vim model matches well with experimental data available in vertical descent but it is extrapolated in the case of descent with forward velocity. More experimental data are needed to update vertical measurements and to extend them to forward descent.

A vortex ring state predicted criterion is elaborated. More experimental data are necessary to obtain more precisely the vortex ring state domain in order to validate this criterion.

In the near future, flight test planed on D6075 will permit:

- to establish the vortex ring state domain in flight,
- to increase experimental data in order to adjust the Vim model.

Induced velocities measurements with probes located on a boom fixed on the D6075 fuselage are also scheduled.

References

[1] VARNES D.J. DUREN R.W. WOOD E.R. An onboard warning system to prevent hazardous "vortex ring state" encounters. In 26^{th} *European Rotorcraft Forum*, pages 88–1, 88–15, The Hague, The Netherlands, September 2000.

[2] WOLKOVITCH Julian. Analytical prediction of vortex-ring boundaries for helicopters in steep descents. *Journal of American Helicopter Society*, Vol.3(No.3):13–19, July 1972.

[3] CASTLES Walter GRAY Robin. Empirical relation between induced velocity, thrust, and rate of descent of a helicopter rotor as determined by wind-tunnel tests on four model rotors. Technical Note 2474, NACA, 1951.

[4] MEIJER DREES IR.J. A theory of airflow throught rotors and its application to some helicopter problems. *Journal of the helicopter society*, 3(No.2), 1949.

[5] BASKIN V.E. VIL'DGRUBE L.S. VOZHDAYEN YE.S. MAYKAPAR G.I. Theory of the lifting airscrew. Technical Translation F-823, NASA, 1976.

[6] PETERS David A. CHEN Shyi-Yaung. Momentum theory, dynamic inflow, and the vortex-ring state. *Journal of American Helicopter Society*, Vol.27(No.3):18–24, July 1982.

[7] HEYSON Harry H. A momentum analysis of helicopters and autogyros in inclined descent, with comments on operational restrictions. Technical Note D-7917, NASA, October 1975.

[8] MEIJER DREES J. HENDAL W.P. The field of flow throught a helicopter rotor obtained from wind tunnel smoke tests. Technical Report A.1205, National Luchtvaart Laboratorum, The Netherlands, 1953.

[9] BROTHERHOOD P. Flow through the helicopter rotor in vertical descent. Technical Report 2735, ARC R&M, 1949.

[10] AZUMA A. OBATA A. Induced flow variation of the helicopter rotor operating in the vortex ring state. *Journal of Aircraft*, Vol.5(No.4), 1968.

[11] WASHIZU K. AZUMA A. K$\bar{O}$O J. OKA T. Experiments on a model helicopter rotor operating in the vortex ring state. *Journal of Aircraft*, Vol.3(No.3), 1966.

[12] NEWMAN S. BROWN R. PERRY J. LEWIS S. ORCHARD M. MODHA A. Comparative numerical and experimental investigations of the vortex ring phenomenon in rotorcraft. In *American helicopter society*, 57^{th} annual forum, May 2001.

[13] XIN H. GAO Z. An experimental investigation of model rotors operating in vertical descent. In *Proceedings of the* 19^{th} *European Rotorcraft Forum*, Cernobbio, Italy, 1993.

[14] INOUE O. HATTORI Y. AKIYAMA K. Calculations of vortex ring states and autorotation in helicopter rotor flow fields. In *American institute of aeronautics and astronautics*, 1997. Paper 97-1847.